Half-metallic ferromagnets. I. Structure and magnetic properties of NiMnSb and related inter-metallic compounds

1989 J. Phys.: Condens. Matter 1 2341

(http://iopscience.iop.org/0953-8984/1/13/007)

J. Phys.: Condens. Matter 1 (1989) 2341–2350. Printed in the UK

Half-metallic ferromagnets: I. Structure and magnetic properties of NiMnSb and related inter-metallic compounds

M J Otto†‡, R A M van Woerden†, P J van der Valk†, J Wijngaard†, C F van Bruggen†, C Haas† and K H J Buschow§

† Laboratory of Inorganic Chemistry, Materials Science Centre, University of Groningen, The Netherlands

§ Philips Research Laboratories, Eindhoven, The Netherlands

Received 15 April 1988, in final form 31 August 1988

Abstract. We present investigations of the crystal structure, the microstructure and the magnetic properties of the inter-metallic compounds XMnSb (X = Pt, Ni, Co, Au, Cu) and PtMnSn. It was found that several of these materials contain precipitates of other phases and/or large atomic disorder, which can be influenced by heat treatment. The magnetic properties show an effective paramagnetic moment which differs from the value corresponding to the saturation moment at 0 K. This effect is attributed to a decrease of the conduction electron spin polarisation at high temperature.

1. Introduction

Since their discovery by Heusler in 1903 (Heusler 1903, Heusler *et al* 1903) the so-called Heusler alloys form an intensively studied class of magnetic materials. One of the reasons is that the crystal structure of these inter-metallic compounds easily allows substitution by many different elements. This makes these compounds most suitable for a study of the relation between chemical composition and magnetic properties.

One can distinguish two types of alloy, with composition XMnZ and X_2MnZ (X = Cu, Ni, Pt, Pd etc, Z = Sb, Sn, In, Ga etc). The XMnZ compounds have been studied to a much lesser extent than the original Heusler alloys X_2MnZ. This changed abruptly after the discovery of the large polar magneto-optic Kerr effect at room temperature in PtMnSb (van Engen *et al* 1983). A large Kerr effect is of importance for optical read-out of magnetically stored information in erasable video and audio discs. The discovery initiated several investigations of the magneto-optical properties of these alloys (van Engen 1983, de Groot *et al* 1984, van Engelen and Buschow 1987, Ohyama *et al* 1987).

A point of special interest is the peculiar band structure of NiMnSb and related compounds (de Groot *et al* 1983). Calculations show that in these compounds the band for minority spin electrons has a gap at the Fermi level, whereas the Fermi level intersects the bands for majority spin electrons. For this reason these materials have been called half-metallic ferromagnets, i.e. they are metallic for electrons with one spin direction and semiconducting for electrons with opposite spin. The band-structure calculations also show that these compounds are good examples of local-moment ferromagnets (de

‡ Present address: Akzo Research BV, Corporate Research Department, Arnhem, The Netherlands.

0953-8984/89/132341 + 10 $02.50

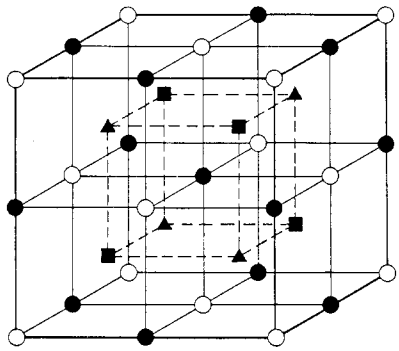

Figure 1. Unit cell of the Heusler structure: ○, A; ■, B; ●, C; ▲, D.

Groot *et al* 1983, Kübler *et al* 1983). The magnetic properties are due to magnetic moments localised at the Mn atoms, interacting via itinerant electrons in a broad conduction band. We expect that the half-metallic character of these materials will also have interesting consequences for the magnetic and the transport properties.

We have investigated the magnetic properties, the transport properties and the electronic structure (Otto *et al* 1989) of several inter-metallic compounds XMnZ. A preliminary account of these studies was published earlier (Otto *et al* 1987), further details are given by Otto (1987). The crystal structure of these compounds allows easily for atomic disorder. In order to obtain reliable and reproducible results the preparation of the samples must be carried out in a careful way. Therefore in this paper we discuss first, in some detail, the preparation and heat treatment and the investigation of the microstructure of the samples used for further investigations. We present experimental data on the magnetic properties. The results are discussed in terms of a simple molecular field model of local moments interacting via itinerant charge carriers (holes) in a broad energy band.

2. Preparation and crystal structure

Polycrystalline ingots of PtMnSb, CoMnSb, NiMnSb, CuMnSb, AuMnSb and PtMnSn were synthesised at 1500 °C by electric-arc melting of the component elements, each of at least 99.99% purity, and subsequent rapid quenching in water. The synthesis was carried out under an atmosphere of pure argon gas.

Another polycrystalline specimen of PtMnSb and a single crystal of PtMnSb were synthesised with the Bridgman method. We also synthesised several specimens of NiMnSb by melting the elements in a high-frequency induction furnace. The elements were placed in an alumina crucible which was subsequently put in a pyrolytic carbon pot with a graphite lid. Fusion occurred at approximately 1050 °C. The temperature of the melt was then increased to 1200 °C. The ingot was cooled, turned upside down and heated again at 1200 °C. This process was repeated four times, in order to obtain a better homogeneity of the sample.

The crystal structure of the Heusler alloys is based on a cubic structure with four interpenetrating FCC lattices A, B, C, D (figure 1). In the completely ordered compounds XYZ the X, Y and Z atoms occupy the A, B and D positions, respectively; the C positions remain unoccupied (Pearson 1958). The compounds NiMnSb (Castelliz 1951, 1952, Helmholdt *et al* 1984, Endo 1970), CuMnSb (Castelliz 1951, 1952, Nowotny and Glatzl 1952, Forester *et al* 1968), AuMnSb (Masumoto and Watanabe 1971) and PtMnSb

Table 1. Crystallographic and magnetic properties of some inter-metallic compounds. The effective moment μ_{eff} is calculated from the Curie constant $C = N\mu_{eff}^2/3k_B$. The paramagnetic Curie temperature is θ, the spontaneous magnetisation is M. The parameters p_C and p_s are defined in the text.

Compound	Unit cell (Å)	Magnetic order	T_C or T_N (K)	$M(T = 0\,K)$ (μ_B)	θ (K)	μ_{eff} (μ_B)	p_C/p_s
CoMnSb	2×5.875	F	478	4.2	490–520	4.6–4.0	0.88–0.74
NiMnSb	5.927	F	728	4.2	780–910	4.2–2.9	0.79–0.49
CuMnSb	6.095	AF	55	3.9	−160	5.4	—
PtMnSb	6.195	F	572	3.96	610–670	4.9–4.3	1.00–0.90
AuMnSb	6.373	F	72	3.5	98	~5.7	~1.3
PtMnSn	6.261	F	330	3.5	350	~5.2	~1.2

(Masumoto and Watanabe 1970, Hames and Crangle 1971) crystallise in this structure ($C1_b$ structure, space group $F\bar{4}3m$). However, the structure easily allows for atomic disorder, either by interchange of atoms or by partial occupancy of the C sites. Moreover, excess atoms are easily incorporated at the C sites, as indicated also by the existence of alloys such as Ni_2MnSb where all A, B, C and D sites are occupied. Because atomic disorder can be influenced by heat treatment, we subjected the samples to several types of heat treatment. For CoMnSb, NiMnSb and PtMnSb annealing during 12 h at 700 °C in a nitrogen atmosphere gave the best ordering.

We determined the crystal structure of our polycrystalline samples using x-ray powder diffraction. The results (diffraction line positions and intensities) generally agree with data reported in the literature. The lattice parameters obtained on our samples are given in table 1. In the completely ordered compounds XYZ, all atoms occupy special positions, and there are no free crystallographic parameters for the positions of the atoms. Therefore the atomic positions are fully determined by the space group and lattice parameters. The line intensities (for details see Otto (1987)) agree approximately in most cases with the ordered distribution, with atoms X, Y, Z occupying sites A, B, D, respectively. Only in the cases of CoMnSb and PtMnSn could a strong atomic disorder be deduced from diffraction line intensities. It was not possible to obtain from the line intensities accurate and reliable quantitative values of the atomic disorder (occupation probabilities of atoms X, Y, Z on A, B, D sites). The composition of the samples was determined by chemical analysis and confirmed with wavelength-dispersive x-ray spectrometry (WDX).

We used several techniques to study the microstructure of the samples. The topography and homogeneity of the polished surface of the samples were investigated with optical microscopy and scanning electron microscopy (SEM), using secondary and backscattered primary electrons for imaging. With energy-dispersive x-ray spectrometry (EDX) differences in atomic composition can be determined with an acuracy of a few per cent. Using WDX a precise atomic composition of a small part of the sample can be obtained. Differential thermal analysis (DTA) and differential scanning calorimetry (DSC) were used to measure phase transitions. Finally we remark that the residual resistivity ρ_0 (resistivity at zero temperature) is a convenient measure of the atomic disorder; in general a large value of ρ_0 indicates a large atomic disorder.

We will describe briefly the results of the investigations of the (micro)structure of the samples.

2.1. Results for individual samples

2.1.1. NiMnSb. X-ray diffraction of a sample of NiMnSb made with an electric arc showed the presence of about 2% NiSb as a second phase. This second phase was also detected with SEM. Samples prepared from equiatomic amounts of the elements in the high-frequency furnace at 1200 °C also showed NiSb x-ray reflections. Annealing during 14 d at 1000 °C and slow cooling decreased the intensities of the NiSb reflections only slightly. Specimens synthesised from the elements with 2% and 3% excess of Mn showed very weak and no NiSb reflections, respectively. This indicates that in NiMnSb about 3% extra Mn is dissolved. However, after polishing, all these samples showed (with SEM) a surface pattern with two types of regions with slightly different Vickers hardness (500 and 460 VH). The nature of these two types of surface is not known. Moreover, the residual resistivity of all samples, mentioned so far, is fairly large ($\rho_0 \simeq 11$–$14 \times 10^{-8}\ \Omega$ m).

We obtained single-phase stoichiometric samples of NiMnSb by synthesis from equiatomic amounts of the elements in an induction furnace at 1200 °C and annealing at 700 °C for 15 d. These samples had a residual resistivity of $7 \times 10^{-8}\ \Omega$ m and showed only NiMnSb x-ray reflections. Moreover, the polycrystalline ingots showed no second phase or surface inhomogeneity with SEM. Differential thermal analysis of these samples showed a sharp melting peak at 1074 °C and a weak anomaly at the Curie temperature.

2.1.2. CoMnSb. Our investigations were carried out on single-phase stoichiometric CoMnSb synthesised by electric-arc melting, followed by annealing four times for a few hours at 430 °C and slow cooling. This procedure was used because from residual resistivity measurements we found that the number of atomic defects decreases strongly as a result of annealing. A SEM image showed a homogeneous sample; with WDX we found atomic ratios of 1 : 1 : 1. DTA scans of annealed CoMnSb showed a sharp melting peak at 1029 °C and a first-order structural phase transition at about 770 °C.

The crystal structure of CoMnSb was first studied by Nowotny and Glatzl (1952), who suggested a C1 structure. On the basis of neutron diffraction data, Natera *et al* (1970) suggested either the $C1_b$ structure (with Co, Mn and Sb at A, B and D sites, respectively), or the $L2_1$ structure (with Co randomly distributed over A and C sites, and Mn and Sb at B and D sites, respectively). From a combined neutron and x-ray diffraction study, Szytula *et al* (1972) concluded that the $L2_1$ structure fits better the data.

Our x-ray diffraction data of the annealed specimen showed more lines than expected for the $L2_1$ or $C1_b$ structures. These lines could be indexed with a doubling of the unit-cell parameters. Such a doubling of the cell parameters was observed by Senateur *et al* (1972). These authors propose a structure with part of the Co atoms distributed randomly. Our resistivity data show a large residual resistivity, of $\rho_0 = 37 \times 10^{-8}\ \Omega$ m, indeed suggesting appreciable atomic disorder.

2.1.3. CuMnSb. According to x-ray diffraction (Castelliz 1951, 1952, Nowotny and Glatzl 1952) and neutron diffraction (Forester *et al* 1968) studies, CuMnSb crystallises in the $C1_b$ structure at 300 K, with Cu on A, Mn on B and Sb on D sites. However, the residual resistivity is quite large, $\rho_0 = 59 \times 10^{-8}\ \Omega$ m, indicating a large atomic disorder. SEM images and EDX measurements showed a homogeneous surface and no phase separations. DTA showed melting at 793 °C, and a phase transition at 480 °C measured with DSC. This transition has an entropy effect of about $R \ln 2$ and could be an order–disorder transition leading to a random distribution of Cu atoms over A and C sites (i.e.,

a $C1_b \rightarrow L2_1$ phase transition).

2.1.4. PtMnSb. Measurements on PtMnSb showed a well ordered homogeneous single-phase stoichiometric $C1_b$ sample (less than 2% Pt–Mn phases). A small residual resistivity of $\rho_0 = 6.8 \times 10^{-8}\ \Omega$ m indicates small atomic disorder. DTA showed melting at 1058 °C.

2.1.5. PtMnSn. The SEM images of PtMnSn showed a homogeneous surface. According to x-ray diffraction, WDX and chemical analysis, the compound is stoichiometric and no second phases are present. The residual resistivity is large, $\rho_0 = 69 \times 10^{-8}\ \Omega$ m, indicating large atomic disorder. This was also concluded from x-ray diffraction studies (Masumoto and Watanabe 1973), which suggested a random distribution of Pt over A and C sites in the annealed sample, and either an ordered or a random distribution of Mn and Sn over B and D sites.

2.1.6. AuMnSb. X-ray diffraction of AuMnSb showed the $C1_b$ structure and in addition a small amount of MnSb indicating that some extra Au atoms are dissolved in the AuMnSb lattice, probably at the C sites. According to SEM and WDX data the surface of the polycrystalline ingots is homogeneous. We could determine the amount of MnSb by magnetic measurements; the result was $4 \pm 1\%$ by weight. This corresponds to a composition $Au_{1+x}MnSb$ with $x = 0.08 \pm 0.02$.

The first DTA heating curve shows a single peak at 574 °C due to melting. On cooling, the corresponding solidification peak (at 578 °C) is much smaller than the melting peak. However, on further cooling a second large peak appears at 515 °C. After this DTA measurement (heating and cooling) EDX measurements showed the presence of three phases in the sample, an Sb phase, a Au–Mn (1 : 1) alloy and a Au–Mn–Sb (1 : 1 : 1) alloy. Apparently the heating–cooling cycle leads to the partial decomposition of AuMnSb.

2.1.7. PtFeSb and PtCrSb. The existence and structure of PtFeSb and PtCrSb were reported in 1983 (Buschow *et al* 1983). The x-ray diffraction patterns of these materials were similar to that of the $C1_b$ structure; however, the presence of extra diffraction lines was taken as evidence for a distorted $C1_b$ structure with lower symmetry.

We have investigated the microstructure of these phases. SEM showed clearly the presence of two phases in the Pt–Fe–Sb sample. From WDX it was found that the compositions of these phases were $PtFe_2$ and $PtSb_2$, and that they were present in about equal amounts. $PtSb_2$ is indeed a stable compound; the diffraction lines reported for PtFeSb correspond closely (angles and intensities) to the diffraction lines of $PtSb_2$. The Pt–Fe phase diagram shows the ordered compounds Pt_3Fe, PtFe and $PtFe_3$. The diffraction lines of these compounds were not observed in the PtFeSb diffraction pattern.

We suggest that $PtFe_2$ is present in microcrystalline form, the particles being too small to give rise to sharp x-ray lines. According to the Pt–Fe phase diagram (Kubaschewski 1982) alloys of the composition $PtFe_2$ undergo an atomic disorder–order transition at a temperature well below the annealing temperature (700 °C) applied when preparing the Pt–Fe–Sb sample. Cooling to room temperature may have led to only a modest degree of ordering since fairly long annealing times below the transformation temperature are required for the latter process. Magnetic measurements on ordered and disordered Pt–Fe alloys in the composition range close to $PtFe_2$ were made by Nakamura *et al* (1979). For the ordered and disordered alloys the Curie temperatures are close to 580 and 460 K, respectively. The latter temperature agrees fairly well with the value

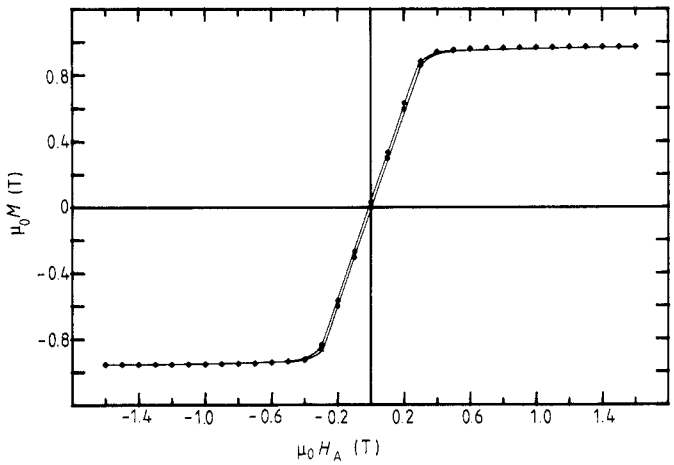

Figure 2. Hysteresis loop of the magnetisation of NiMnSb at 292 K.

(430 K) found in the Pt–Fe–Sb sample. We conclude that the compound PtFeSb does not exist, and that the sample described in the literature is in fact a two-phase system, consisting of crystalline $PtSb_2$ and a microcrystalline $PtFe_2$ phase.

SEM images of the PtCrSb sample showed the presence of several phases, the composition of which was determined with WDX. We observed the phases CrSb, $PtCr_3$, PtCr and $PtSb_2$. These phases were also found with x-ray diffraction. Our conclusion is that the compound PtCrSb also does not exist.

3. Magnetic properties

The magnetisation was measured as a function of the temperature and applied magnetic field. For the temperature region 4–300 K we used a Faraday balance with superconducting magnet (magnetic field 0–4 T). For measurements between 300 and 900 K we used a Foner vibrating sample magnetometer with a Bruker electromagnet (−1.6 to +1.6 T). For susceptibility measurements between 300 and 1200 K a homemade Faraday system was used (van Bruggen 1969). The absolute accuracy of the magnetic measurements is generally of the order of 1%; the scattering of the points in the figures gives a good indication of the relative precision.

The inter-metallic compounds PtMnSb, NiMnSb, CoMnSb, AuMnSb and PtMnSn are ferromagnets. CuMnSb is an antiferromagnet with a low Néel temperature (Endo 1970) and magnetic moments of about 4 μ_B at the Mn atoms (Forester *et al* 1968). In figure 2 the hysteresis loop of NiMnSb is shown; this curve is representative for all ferromagnetic alloys studied. The coercive field is very small, about 0.005 T.

The spontaneous magnetisation $M(T)$ as a function of temperature of the ferromagnetic compounds is shown in figure 3. The magnetisation values were obtained by properly taking into account the effect of the applied and the demagnetising field. The measurements for AuMnSb were corrected for the contribution of a few per cent of ferromagnetic MnSb present in the sample. A quantitative correction of the magnetisation for the effect of MnSb is quite possible, so values of $M(T)$ for AuMnSb are believed to be reliable. However, the correction for susceptibility measurements is more difficult and the values for the susceptibility of AuMnSb could have a large experimental error.

The curves of the spontaneous magnetisation against temperature are close to a

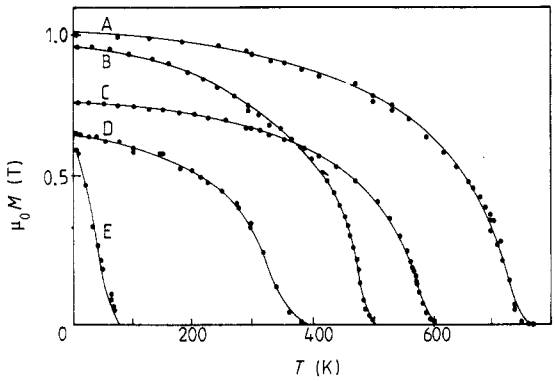

Figure 3. Spontaneous magnetisation M as a function of temperature: A, NiMnSb; B, CoMnSb; C, PtMnSb; D, PtMnSn; E, AuMnSb.

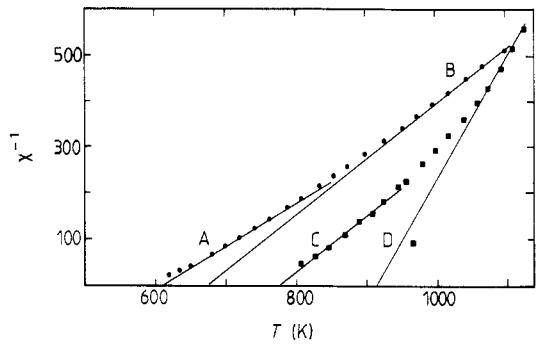

Figure 4. Inverse magnetic susceptibility of PtMnSb (●) and NiMnSb (■): A, $\mu_{eff} = 4.9\ \mu_B$; B, $\mu_{eff} = 4.3\ \mu_B$; C, $\mu_{eff} = 4.2\ \mu_B$; D, $\mu_{eff} = 2.9\ \mu_B$.

Brillouin function at higher temperature. At low temperature the curves for PtMnSb and CoMnSb follow the expression $M(T) = M(0)(1 - AT^n)$ with $n = 1.5$, the value expected from spin-wave theory. The values of A are $2.3 \times 10^{-5}\ K^{-3/2}$ and $2.1 \times 10^{-5}\ K^{-3/2}$ for CoMnSb and PtMnSb, respectively. For NiMnSb a deviating behaviour with $n = 1.9$ was observed, while for PtMnSn a value of $n = 1.2$ was found. With spin-wave theory we can calculate the value of the spin-wave stiffness coefficient D in the spin-wave dispersion relation $\hbar\omega = Dq^2$ from the value of A, using the equation (Marshall and Lovesey 1971) $A = 2.612(V/S)(k_B/4\pi D)^{3/2}$. ($V$ is the volume per magnetic atom, S is the spin and k_B is the Boltzmann constant.) The values obtained are $D = 134$ meV Å^2 and $D = 164$ meV Å^2 for CoMnSb and PtMnSb, respectively. The deviating value of n for NiMnSb indicates a strong temperature dependence $D = D_0 - D_1T^2$. The experimental data of A for NiMnSb are well reproduced between 4 and 330 K with the values $D_0 = 350 \pm 40$ meV Å^2 and $D_1 = (15 \pm 7) \times 10^{-4}$ meV Å^2 K^{-2}. The low value of n for PtMnSn could be due to perturbation of spin-wave propagation by disorder in the spatial distribution of magnetic moments, caused by Mn–Sn atomic disorder.

The magnetic susceptibility above the Curie (or Néel) temperature does not show Curie–Weiss behaviour. The effective magnetic moment μ_{eff}, deduced from the slope of a χ^{-1} against T plot, decreases with increasing temperature; at the same time the extrapolated intercept θ changes (see figure 4). For PtMnSb the values of μ_{eff} and θ change from 4.9–4.3 μ_B and 610–670 K in the temperature region 700–1100 K. For NiMnSb the variation is even stronger, with $\mu_{eff} = 4.2\ \mu_B$, $\theta = 780$ K near 800 K, and $\mu_{eff} = 2.9\ \mu_B$, $\theta = 910$ K near 1120 K. The corresponding values for CoMnSb are $\mu_{eff} = 4.6\ \mu_B$, $\theta = 490$ K near 550 K, and $\mu_{eff} = 4.0\ \mu_B$, $\theta = 520$ K near 700 K. A survey of the magnetic data is given in table 1. The observed values of the Curie temperature and

the saturation magnetisation are generally in agreement with data in the literature of CoMnSb (Natera *et al* 1970, Szytula *et al* 1972), NiMnSb (van Engen *et al* 1983, Helmholdt *et al* 1984, Szytula *et al* 1972), CuMnSb (Endo 1970, Forester *et al* 1968), PtMnSb (van Engen *et al* 1983, Masumoto and Watanabe 1970, Hames and Crangle 1971, Watanabe 1976), AuMnSb (Masumoto and Watanabe 1971) and PtMnSn (van Engen *et al* 1983, Hames and Crangle 1971, Masumoto and Watanabe 1973). Small differences are probably due to differences in stoichiometry and thermal treatment (atomic disorder) of the samples.

The observed magnetic moments in all the investigated Heusler alloys are about $4\,\mu_B$. As indicated by band-structure calculations and by neutron diffraction data for NiMnSb (Helmholdt *et al* 1984) and CuMnSb (Forester *et al* 1968), local magnetic moments are only present at the Mn atoms, except for a small moment on Co in CoMnSb (Natera *et al* 1970, Szytula *et al* 1972). A similar situation occurs in the X_2MnZ-type Heusler alloys (X = Ni, Co, Pd, Cu and Z = Al, Si, Ge, Ga, In, Sb, Sn). Also in these materials the magnetic moments are localised at the Mn atoms (Felcher *et al* 1963, Webster and Tebble 1968), but in Co_2MnSb there is also a moment on Co. Results of inelastic neutron scattering on Ni_2MnSn and Pd_2MnSn (Noda and Ishikawa 1976) also indicate that Heusler alloys are good examples of local-moment ferromagnets.

In addition to the local moments there are the spin-polarised holes in the broad Sb 5p valence band in NiMnSb and PtMnSb (de Groot *et al* 1983). The distances between the localised Mn moments are too large for a strong direct-exchange interaction. Therefore one expects the ferromagnetic coupling to be effected mainly by the itinerant holes. This coupling mechanism also explains the low magnetic transition temperatures in CuMnSb and AuMnSb (see table 1). These compounds have one electron more than NiMnSb and PtMnSb, and the Sb 5p band will be (nearly) completely filled and hence not effective for indirect ferromagnetic exchange between the Mn magnetic moments. This argument also explains the difference in magnetic properties between PdMnSb (ferromagnetic with $T_C = 500$ K (Hames 1960)) and PdMnTe (antiferromagnetic with $T_N = 17$ K (Masumoto *et al* 1974)).

An unusual property of CoMnSb, NiMnSb and PtMnSb is the small value of the effective magnetic moment above T_C and its decrease with increasing temperature. For these compounds the Rhodes–Wohlfarth ratio p_C/p_s is less than unity (see table 1); p_s refers to the saturation moment $p_s\mu_B$ (at $T = 0$ K), and p_C to the effective moment per magnetic atom deduced from the Curie constant $C = N\mu_B^2 p_C(p_C + 2)/3k_B$. This behaviour is very unusual: for local-moment ferromagnets one expects a ratio $p_C/p_s = 1$; for itinerant ferromagnets (Stoner model) one expects a ratio $p_C/p_s > 1$ (Rhodes and Wohlfarth 1963, Wohlfarth 1978). Since neither the itinerant nor the localised model explains a ratio $p_C/p_s < 1$, we propose a simple molecular field model, which takes into account both local moments and spin-polarised itinerant electrons, to explain the observed ratio $p_C/p_s < 1$.

The total magnetisation $M = M_1 + M_2$ has contributions from the local moments M_1 and from the itinerant holes M_2. The magnetisation induced by an applied magnetic field H at a temperature above T_C is given by

$$M_1 = (C_1/T)(\lambda_{11}M_1 + \lambda_{12}M_2 + H) \tag{1}$$

$$M_2 = \chi_P(\lambda_{21}M_1 + \lambda_{22}M_2 + H) \tag{2}$$

where $C_1 = Ng^2\mu_B^2 S_0(S_0 + 1)$ is the Curie constant of the local moments with spin S_0, χ_P is the Pauli susceptibility of the holes and λ_{ij} are the coupling constants. From these equations we obtain for the total susceptibility

$$\chi = C_1(1 + \gamma\chi_P\lambda_{12})^2/(T - \theta) + \gamma\chi_P \tag{3}$$

with $\gamma = (1 - \lambda_{22}\chi_P)^{-1}$ and $\theta = C_1(\lambda_{11} + \gamma\lambda_{12}^2\chi_P)$. Therefore, in addition to an enhanced temperature-independent Pauli susceptibility, $\gamma\chi_P$, we obtain a Curie–Weiss law with an effective Curie constant $C_{eff} = C_1(1 + \gamma\lambda_{12}\chi_P)^2$. The Curie constant is reduced if the interaction between local moments and holes is antiferromagnetic ($\lambda_{12} < 0$).

The saturation magnetisation at $T = 0$ K is also reduced due to the negative spin polarisation of the holes. The value of M_2 at $T = 0$ K, obtained from (2) for $H = 0$, is

$$M_2(0\text{ K}) = -\beta M_1(0\text{ K}) \tag{4}$$

with $\beta = -\gamma\lambda_{12}\chi_P$ and $M_1(0\text{ K}) = Ng\mu_B S_0$. This equation is not valid if β is large; in that case M_2 saturates at the value $-p\mu_B$ (p is the hole concentration). Therefore the total saturation magnetisation at $T = 0$ K is given by

$$M(0\text{ K}) = Ng\mu_B S_0(1 - \beta) \qquad \text{for } \beta < p/NgS_0 \tag{5}$$

and

$$M(0\text{ K}) = Ng\mu_B S_0 - p\mu_B \qquad \text{for } \beta > p/NgS_0. \tag{6}$$

The Rhodes–Wohlfarth ratio p_C/p_s is easily calculated from these equations. We find for $\beta < (p/NgS_0)$ values of p_C/p_s slightly less than unity, but for $\beta > (p/NgS_0)$ a strong reduction of p_C/p_s. For example, for NiMnSb, with $S_0 = \frac{5}{2}$, $g = 2$, $p = N$, we obtain $M(0\text{ K}) = 5N(1 - \beta)\mu_B$ for $\beta > 0.2$ and p_C/p_s values varying from 1 for $\beta = 0$ to $p_C/p_s = 0.93$ for $\beta = 0.2$. For $\beta > 0.2$ we obtain $M(0\text{ K}) = 4N\mu_B$, and $p_C/p_s = 0.82$ and 0.67 for $\beta = 0.3$ and 0.4, respectively. We remark that with $S_0 = \frac{5}{2}$ and $p = N$ only cases with $\beta \geqslant 0.2$ correspond to a half-metallic ferromagnet, so that for NiMnSb we expect $\beta \geqslant 0.2$. We conclude that p_C/p_s values less than unity are expected for all values of β, but particularly small values of p_C/p_s are expected for half-metallic ferromagnets (with $\beta \geqslant 0.2$).

Finally we try to show that a value of $\beta \simeq 0.2$ for NiMnSb is reasonable. The dominant exchange interaction in NiMnSb is the interaction λ_{12} between local moments and itinerant holes. If we neglect the direct interaction λ_{11}, the Curie temperature is given by $T_C = C_{11}\gamma\chi_P\lambda_{12}^2$. An estimate for χ_P can be obtained from band-structure calculations. The holes in NiMnSb occupy the top of the Sb 5p band; the Fermi energy in the fully spin-polarised state is $E_F = 1.9$ eV (de Groot *et al* 1983). This corresponds to a Fermi energy of the unpolarised state $E_{F0} = 2^{-2/3}E_F = 1.2$ eV. With $\chi_P = p\mu_B^2/E_F$ we obtain $\chi_P = 0.9 \times 10^{-6}$. Substituting $T_C = 728$ K and the value of C_{11}, we find for NiMnSb $\lambda_{12} = 8 \times 10^4\,\gamma^{-1/2}$ and $\beta = 0.07\gamma^{1/2}$. The value of γ is difficult to calculate. However, these estimates show that a value of $\beta \simeq 0.2$ for NiMnSb is not unreasonable.

We observed for AuMnSb and PtMnSn a p_C/p_s value greater than unity. For AuMnSb this is probably due to the weak coupling λ_{12} between holes and local moments, as indicated also by the low value of T_C for AuMnSb. The case of PtMnSn is more complicated. According to band-structure calculations, this material is not a half-metallic ferromagnet, but it has holes in both spin sub-bands (de Groot *et al* 1983).

Acknowledgments

Polycrystalline PtMnSb and single-crystal NiMnSb, synthesised by the Bridgman method, were kindly provided by Dr Z Fisk, Los Alamos National Laboratory, USA. We gratefully acknowledge Dr G Boom of the Department of Applied Physics, Groningen, The Netherlands, who put at our disposal the analytical facilities SEM, EDX and

WDX, and assisted in interpreting the data obtained. This investigation was supported by the Netherlands Foundation for Chemical Research (SON) with financial aid from the Netherlands Organisation for the Advancement of Pure Research (ZWO).

References

Buschow K H J, Van Vucht J H N, van Engen P G, de Mooij D B and van der Kraan A M 1983 *Phys. Status Solidi* a **75** 617
Castelliz L 1951 *Monatsh. Chem.* **82** 1059
—— 1952 *Monatsh. Chem.* **83** 1314
de Groot R A, Mueller F M, van Engen P G and Buschow K H J 1983 *Phys. Rev. Lett.* **50** 2024
—— 1984 *J. Appl. Phys.* **55** 2151
Endo K 1970 *J. Phys. Soc. Japan* **29** 643
Felcher G P, Cable J W and Wilkinson M K 1963 *J. Phys. Chem. Solids* **24** 1663
Forester R H, Johnston G B and Wheeler D A 1968 *J. Phys. Chem. Solids* **29** 855
Hames F A 1960 *J. Appl. Phys.* **31** Suppl. S370
Hames F A and Crangle J 1971 *J. Appl. Phys.* **42** 1336
Helmholdt R B, de Groot R A, Mueller F M, van Engen P G and Buschow K H J 1984 *J. Magn. Magn. Mater.* **43** 249
Heusler F 1903 *Verhandl. Deuts. Phys. Ges.* **5** 219
Heusler F, Stark W and Haupt E 1903 *Verhandl. Deuts. Phys. Ges.* **5** 220
Kubaschewski O 1982 *Iron–Binary Phase Diagrams* (Berlin: Springer)
Kübler J, Williams A R and Sommers C B 1983 *Phys. Rev.* B **28** 1745
Marshall W and Lovesey S 1971 *Theory of Thermal Neutron Scattering* (Oxford: OUP)
Masumoto H and Watanabe K 1970 *Trans. Japan Inst. Met.* **11** 385
—— 1971 *Trans. Japan Inst. Met.* **12** 256
—— 1973 *Trans. Japan Inst. Met.* **14** 408
Masumoto H, Watanabe K and Ohnuma S 1974 *Trans. Japan Inst. Met.* **15** 135
Nakamura Y, Sumiyama K and Shiga M 1979 *J. Magn. Magn. Mater.* **12** 127
Natera M G, Murthy M R L N, Begum R J and Satya Murthy N S 1970 *Phys. Status Solidi* a **3** 959
Noda Y and Ishikawa Y 1976 *J. Phys. Soc. Japan* **40** 699
Nowotny H and Glatzl B 1952 *Monatsh. Chem.* **83** 237
Ohyama R, Koyanagi T and Matsubara K 1987 *J. Appl. Phys.* **61** 2347
Otto M J 1987 *PhD Thesis* Groningen University
Otto M J, Feil H, van Woerden R A M, Wijngaard J, van der Valk P J, van Bruggen C F and Haas C 1987 *J. Magn. Magn. Mater.* **70** 33
Otto M J, van Woerden R A M, van der Valk P J, Wijngaard J, van Bruggen C F and Haas C 1989 *J. Phys.: Condens. Matter* **1** 2351–60
Pearson W B 1958 *Handbook of Lattice Spacings and the Structure of Metals* (London: Pergamon)
Rhodes P and Wohlfarth E P 1963 *Proc. R. Soc.* A **273** 247
Senateur J P, Rouault A, Fruchart R and Fruchart D 1972 *J. Solid State Chem.* **5** 229
Szytula A, Dimitrijevic Z, Todorovic T, Kolodziejczyk A, Szelag J and Wanic A 1972 *Phys. Status Solidi* a **9** 97
van Bruggen C F 1969 *PhD Thesis* Groningen University
van Engelen P P J and Buschow K H J 1987 *Philips J. Res.* **42** 429
van Engen P G 1983 *PhD Thesis* Delft University
van Engen P G, Buschow K H J, Jongebreur R and Erman M 1983 *Appl. Phys. Lett.* **42** 202
Watanabe K 1976 *Trans. Japan Inst. Metals* **17** 220
Webster P J and Tebble R S 1968 *Phil. Mag.* **16** 347
Wohlfarth E P 1978 *J. Magn. Magn. Mater.* **7** 113